Volume 1 | Number 1 | Jan 2013 | Pages 1–100

Soft Matter

www.rsc.org/softmatter

ROYAL SOCIETY OF CHEMISTRY

ROYAL SOCIETY OF CHEMISTRY

www.rsc.org/softmatter

Original paper for Soft Matter

Preparation of upper critical solution temperature (UCST) responsive diblock copolymers bearing pendant ureido groups and their micelle formation behavior in water†

Ami Fujihara,[a] Naohiko Shimada,[b] Atsushi Maruyama,[b] Kazuhiko Ishihara,[cd] Keita Nakai,[a] and Shin-ichi Yusa*[a]

[a] Department of Materials Science and Chemistry, University of Hyogo, 2167 Shosha, Himeji, Hyogo 671-2280, Japan. E-mail: yusa@eng.u-hyogo.ac.jp

[b] Graduate School of Bioscience and Biotechnology, Tokyo Institute of Technology, 4259 Nagatsuta-cho, Midori-ku, Yokohama, Kanagawa, 226-8501 Japan

[c] Department of Materials Engineering, [d]Department of Bioengineering, School of Engineering, The University of Tokyo, 7-3-1 Hongo, Bunkyo-ku, Tokyo 113-8656, Japan

ABSTRACT

Poly(2-ureidoethyl methacrylate) (PUEM) was prepared via reversible

addition-fragmentation chain transfer (RAFT) controlled radical polymerization and post-modification reaction. PUEM shows upper critical solution temperature (UCST) behavior in aqueous solution. Although PUEM can dissolve in water above the UCST, it cannot dissolve in water below the UCST. Diblock copolymers (M_mU_n) composed of a biocompatible hydrophilic poly(2-methacryloyloxyethyl phosphorylcholine) (PMPC) block and a PUEM block with different compositions were prepared via RAFT radical polymerization and post-modification reaction. "M" and "U" represent PMPC and PUEM blocks, respectively, and the subscripts represent degree of polymerization of each block. $M_{95}U_{149}$ and $M_{20}U_{163}$ formed polymer micelles comprising a PUEM core and PMPC shell below the critical aggregation temperature (T_c) in aqueous solution. Polymer micelles were formed from $M_{20}U_{163}$ below 32 °C, which can incorporate guest molecules into the core.

1. Introduction

The properties of solubility, viscosity, and wettability for stimuli-responsive polymers can be changed reversibly by various kinds of external stimuli including pH, temperature, and light. In recent years, much effort has been focused on the development of these "intelligent materials."[1-6] Although the polymer in these systems

2

can dissolve in solution below a certain temperature, it does not dissolve above that temperature. The point at which this occurs is referred to as the lower critical solution temperature (LCST). In contrast, the polymer can dissolve in solution above a certain temperature, which is the upper critical solution temperature (UCST). Poly(N-isopropylacrylamide) (PNIPAM) shows LCST behavior in water.[7,8] Below the LCST (32 °C), PNIPAM can dissolve in water due to hydrogen bonding interactions between the pendant amide groups and water molecules. At > 32 °C, macroscopic phase separation of the solution can be observed due to dehydration of the polymer chains. The hydrogen bonding interactions are broken by thermally enhanced molecular motions.

Some UCST behaviors are induced by intra- and inter-hydrogen bonding interactions, which can be observed in organic solvents and mixed solvents of water and organic solvent.[9-11] Poly(N-(4-vinylbenzyl)-N,N-dimethylamide) exhibits UCST behavior in 2-propanol, which depends on its degree of polymerization (DP).[12] UCST-type polymers in water without organic solvents are rare. Woodfield et al.[13] reported that random copolymers composed of zwitterionic 3-((3-aminopropyl) dimethylammonio) propane-1-sulfonate and benzylacrylamide show UCST behavior in water. Below the UCST, the random copolymer cannot dissolve in water, because the

3

anionic and cationic charges in the zwitterionic copolymer interact with each other. The

random copolymer can dissolve in water above the UCST, because the electrostatic

interactions of zwitterionic charges are broken by thermally enhanced molecular

motions. Seuring et al.[14] reported that nonionic poly(methacrylamide) homopolymers

and random copolymers of acrylamide and acrylonitrile,

poly(acrylamide-*co*-acrylonitrile) (P(AAm-*co*-AN)) show UCST behavior in water.

Both poly(methacrylamide) and P(AAm-*co*-AN) have hydrogen bonding donors and

accepters within the pendant groups, which cannot dissolve in water below certain

temperatures to form complexes due to the formation of hydrogen bonds. At elevated

temperatures, these polymers can dissolve in water, because the hydrogen bonds are

broken.

Shimada and Maruyama et al.[15,16] reported that pendant ureido groups-bearing

poly(allylamine-*co*-allylurea) shows UCST behavior in water under physicobiological

conditions. The ureido group has a high number of hydrogen bonding sites.[17] Therefore,

resonance structures of the ureido group contribute to enhance the hydrogen bonding.[18]

Formation of dimers and aggregates of urea in water is suggested by osmotic pressure

and spectroscopic measurements.[19-21] UCST behavior of the polymer with pendant

ureido groups may be related to self-association of urea in water. The UCST of pendant

ureido groups-bearing polymers can be controlled by their molecular weight, content of

ureido groups, polymer concentration, and concentration of added salt in the aqueous

solution.

Amphiphilic diblock copolymers composed of hydrophobic and hydrophilic

block segments spontaneously form polymer micelles composed of a hydrophobic core

covered with a hydrophilic shell in water above the critical aggregation concentration. If

the stimuli-responsive polymer is applied as a hydrophobic block segment in

amphiphilic diblock copolymers, the association behavior can be controlled by external

stimuli.[22,23] Diblock copolymers (PNIPAM-*b*-PNVP) composed of thermo-responsive

PNIPAM and hydrophilic poly(*N*-vinylpyrrolidone) (PNVP) can dissolve in water as a

unimer state below the LCST for the PNIPAM block.[24] Above the LCST, the diblock

copolymers form polymer micelles comprised of a dehydrated PNIPAM core and

hydrophilic PNVP shell. These thermo-responsive association behaviors are completely

reversible. Poly(methacrylic acid)-*block*-poly((*N,N*-diethylamino)ethyl methacrylate)

(PMAA-*b*-PDEA) exhibits pH-responsive association behavior in water. Under acidic

conditions, pH 3, the PMAA block is hydrophobic due to protonation of the pendant

carboxyl groups, and the PDEA block is hydrophilic due to ionization of the pendant

tertiary amino groups.[25] The diblock copolymers form micelles in water composed of a

5

hydrophobic PMAA core and hydrophilic PDEA shell at pH 3. Under basic conditions,

pH 12, the diblock copolymers form polymer micelles composed of a dehydrated PDEA

core and ionized PMAA shell. Zhan et al.[26] reported that three kinds of

thermo-responsive diblock copolymers which have a UCST-type random copolymer

block of P(AAm-*co*-AN) coupled with hydrophobic polystyrene (PS) or hydrophilic

poly(*N,N*-dimethylacrylamide) (PDMA) or a LCST polymer of

poly(*N,N*-dimethylaminoethyl methacrylate) (PDMAEMA) were prepared via

reversible addition-fragmentation chain transfer (RAFT) controlled radical

polymerization. These diblock copolymers show thermo-responsive association

behavior in water based on the UCST behavior of the uncharged P(AAm-*co*-AN) block.

The phosphorylcholine group of 2-methacryloyloxyethyl phosphorylcholine

(MPC) has the same chemical structure as the hydrophilic portion of cell

membranes.[27-29] Water-soluble MPC can be polymerized with other vinyl compounds,

and the properties and functions of such polymers can be controlled by choosing an

appropriate comonomer. MPC polymer (PMPC) shows excellent biocompatibility and

antithrombogenicity. Polymer micelles covered with biocompatible PMPC shells may

be an excellent candidate as a carrier for a drug delivery system (DDS).

In this study, poly(2-ureidoethyl methacrylate) (PUEM) was prepared via

RAFT radical polymerization and post-modification reaction. UCST behavior of PUEM was studied in 0.1 M NaCl aqueous solution. Diblock copolymers (M_mU_n) composed of a biocompatible water-soluble PMPC block and UCST-type PUEM block were prepared via RAFT radical polymerization and post-modification reaction (Fig. 1). "M" and "U" represent PMPC and PUEM blocks, respectively, and the subscripts represent DP of each block. Above the critical aggregation temperature (T_c), M_mU_n can dissolve in water as a unimer state, because both PMPC and PUEM blocks are hydrophilic. In contrast, below T_c, M_mU_n forms polymer micelles comprising a PUEM core and hydrophilic PMPC shell in water. The thermo-responsive association behavior was reversible. It is expected that the micelle formed at $< T_c$ has a stealth nature against the immune system in the body, because the surface of the micelle may be covered with biocompatible PMPC shells. The PUEM core can incorporate guest molecules at $< T_c$. The polymer micelles can be applied as a thermo-responsive carrier for DDS, because the polymer micelles can release their contents from the core to bulk water above T_c due to dissociation of the micelles.
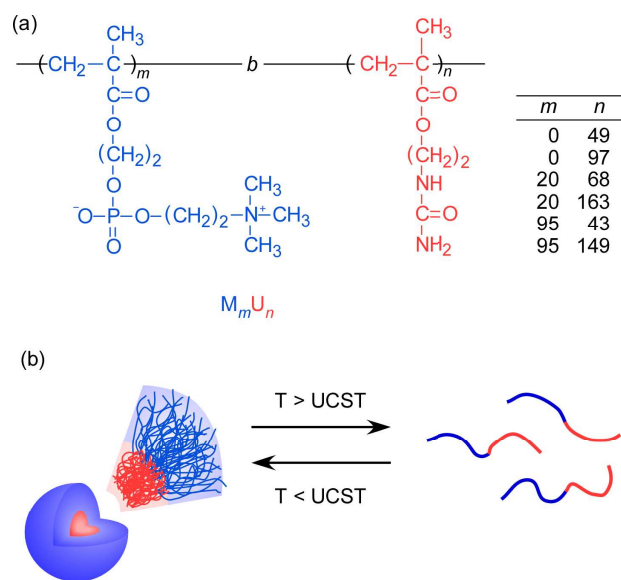
Fig. 1 (a) Chemical structure of diblock copolymers (M_mU_n). (b) Schematic representation of thermo-responsive aggregation behavior of the diblock copolymers in aqueous solution.

2. Experimental section

2.1 Materials

2-Methacryloyloxyethyl phosphorylcholine (MPC) was synthesized as previously reported and recrystallized from acetonitrile.[30] 2-Aminoethyl methacrylate hydrochloride (AEM, 95%, Polyscience, Inc.), 4,4'-azobis(4-cyanovaleric acid) (V-501, 98%, Wako Pure Chemical), potassium cyanate (98%, Wako Pure Chemical), *N*-phenyl-1-naphthylamine (PNA, 98%, Tokyo Chemical Industry), and bovine serum albumin (BSA, > 95%, Wako Pure Chemical) were used as received. 4-Cyanopentanoic

acid dithiobenzoate (CPD) was synthesized as previously reported.[31] Methanol was

dried over 4 Å molecular sieves and purified by distillation. Imidazole buffer was

prepared using 1 M imidazole aqueous solution adjusted to pH 6.0 by hydrochloric acid.

Phosphate buffered saline (PBS) tablet (Sigma Aldrich) was used as dissolved one tablet

in 200 mL of pure water. Water was purified with a Millipore Milli-Q system.

2.2 Synthesis of poly(2-aminoethyl methacrylate hydrochloride) (PAEM$_n$)

AEM (0.995 g, 6.01 mmol), CPD (16.9 mg, 6.01×10^{-2} mmol), and V-501 (6.73 mg,

2.40×10^{-2} mmol) were dissolved in a mixed solvent of imidazole buffer and methanol

(4.0 mL, 8/2, v/v). The solution was deoxygenated by purging with Ar gas for 30 min.

Polymerization was carried out at 70 °C for 4 h. After cooling to room temperature, a

part of the polymerization mixture was analyzed using ^{1}H NMR to determine the

conversion (97.0%). The reaction mixture was dialyzed against pure water for one day.

The polymer (PAEM$_{97}$) was recovered by a freeze-drying technique (0.742 g, 74.6%).

DP and number-average molecular weight (M_n(theo)) estimated from conversion were

97 and 1.61×10^4, respectively. The molecular weight distribution (M_w/M_n) estimated

from gel-permeation chromatography (GPC) was 1.17. PAEM$_{49}$ was prepared similar

procedure of preparation and purification of PAEM$_{97}$. The conversion was 97.6% as

estimated from ^{1}H NMR analysis. DP and M_n(theo) estimated from conversion were 49

and 5.56×10^3, respectively. M_w/M_n estimated from GPC was 1.19.

2.3 Synthesis of poly(2-ureidoethyl methacrylate) (PUEM$_n$)

PAEM$_{97}$ (0.729 g, 4.54×10^{-2} mmol, M_n(theo) $= 1.61 \times 10^4$, $M_w/M_n = 1.17$) and

potassium cyanate (0.358 g, 4.41 mmol) were dissolved in imidazole buffer (8.8 mL).

The solution was stirred at room temperature for 4 h. The reaction mixture was dialyzed

against pure water for two days. The polymer (PUEM$_{97}$) was recovered by a

freeze-drying technique (0.296 g, 39.1%). PUEM$_{49}$ was prepared similar procedure of

preparation and purification of PUEM$_{97}$. The synthetic route of PUEM$_n$ is shown in the

ESI (Fig. S1†).

2.4 Synthesis of poly(2-methacryloyloxyethyl phosphorylcholine) (PMPC$_m$)

MPC (10.8 g, 36.7 mmol), CPD (94.7 mg, 0.339 mmol), and V-501 (47.6 mg, 0.170

mmol) were dissolved in a mixed solvent of water and methanol (36.8 mL, 8/2, v/v).

The solution was deoxygenated by purging with Ar gas for 30 min. Polymerization was

carried out at 70 °C for 4 h. After cooling to room temperature, a part of the

polymerization mixture was analyzed using ^{1}H NMR to determine the conversion

(100%). The reaction mixture was dialyzed against pure water for two days. The

polymer (PMPC$_{95}$) was recovered by a freeze-drying technique (9.30 g, 85.0%). DP and

M_n(theo) estimated from ^{1}H NMR were 95 and 3.22 × 10^4, respectively. M_w/M_n

estimated from GPC was 1.15. PMPC$_{20}$ was prepared by a similar method as described

above. DP, M_n(theo), and M_w/M_n for PMPC$_{20}$ were 20, 6.18 × 10^3, and 1.13,

respectively.

2.5 Synthesis of poly(2-methacryloyloxyethyl phosphorylcholine)-*block*-poly(2-aminoethyl methacrylate hydrochloride) (M$_m$A$_n$)

A typical procedure for block copolymerization is as follows: AEM (1.17 g, 7.07 mmol),

PMPC$_{95}$ (1.00 g, 3.54 × 10^{-2} mmol, M_n(theo) = 3.22 × 10^4, M_w/M_n = 1.15), and V-501

(4.96 mg, 1.77 × 10^{-2} mmol) were dissolved in imidazole buffer (10.4 mL). The solution

was deoxygenated by purging with Ar gas for 30 min. Polymerization was carried out at

70 °C for 2 h. After cooling to room temperature, a part of the polymerization mixture

was analyzed using ^{1}H NMR to determine the conversion (74.8%). The reaction mixture

was dialyzed against pure water for two days. The diblock copolymer (M$_{95}$A$_{149}$) was

recovered by a freeze-drying technique (1.65 g, 75.9%). DP for the PAEM block and

M_n(theo) for the diblock copolymer estimated from ^{1}H NMR were 149 and 5.30 × 10^4,

11

respectively. M_w/M_n estimated from GPC was 1.21.

2.6 Synthesis of poly(2-methacryloyloxyethyl phosphorylcholine)-*block*-poly(2-ureidoethyl methacrylate) (M_mU_n)

A typical procedure for preparation of $M_{95}U_{149}$ is as follows: $M_{95}A_{149}$ (0.803 g, 1.50×10^{-2} mmol, M_n(theo) $= 5.30 \times 10^4$, $M_w/M_n = 1.21$) and potassium cyanate (0.270 g, 3.33 mmol) were dissolved in imidazole buffer (11 mL). The solution was stirred at 50 °C for 28 h. The reaction mixture was dialyzed against pure water for two days. The diblock copolymer ($M_{95}U_{149}$) was recovered by a freeze-drying technique (0.692 g, 86.0%). The synthetic route of M_mU_n is shown in the ESI (Fig. S2†).

2.7 Measurements

^{1}H NMR spectra were obtained with a Bruker DRX-500 NMR spectrometer operating at 500 MHz. ^{1}H NMR sample solutions were prepared in D_2O and D_2O containing 0.1% NaOD. GPC measurements for $PMPC_m$ were performed using a Tosho RI8020 refractive index (RI) detector equipped with a Tosoh DP8020 pump and a Shodex Asahipak SB-804 HQ column. An aqueous phosphate buffer (50 mM, pH 8) containing 10 vol% acetonitrile was used as the eluent at a flow rate of 0.6 mL/min at 40 °C.

M_n(GPC) and M_w/M_n of the samples were calibrated using poly(sodium styrenesulfonate) standards. GPC measurements for PAEM$_{97}$ and M$_m$A$_n$ were performed using a Jasco RI-2031 plus RI detector equipped with a Jasco PU-2080 pump and a Shodex OHpak SB-G and SB-804HQ column. A 0.3 M Na$_2$SO$_4$ aqueous solution containing 0.5 M acetic acid was used as the eluent at a flow rate of 0.6 mL/min at 40 °C. M_n(GPC) and M_w/M_n were calibrated using poly(2-vinylpyridine) standards. Percent transmittance (*%T*) measurements were performed using a Jasco V-630 BIO UV-vis spectrometer with a 10 mm path length quartz cell. The temperature was decreased from 60 to 10 °C and increased from 10 to 60 °C with cooling and heating rates of 1.0 °C/min with a Jasco ETC-717 thermostat system. Dynamic light scattering (DLS) measurements were performed using a Malvern Zetasizer nano ZS equipped with a He-Ne laser (4 mW at 632.8 nm). The polymer concentration (C_p) was kept constant at 5.0 g/L unless otherwise noted. Polymers were dissolved in NaCl aqueous solution and stirred overnight at 60 °C. DLS measurements were performed changing the temperature from 60 to 10 °C. Hydrodynamic radius (R_h) was calculated by a cumulant analysis method. R_h distributions were obtained by a non-negatively constrained least squares (NNLS) analysis method. The details of DLS instrumentation and theory are described in the literature.[32,33] Static light scattering (SLS) measurements were

13

performed on an Otsuka Electronics Photal DLS-7000DL light scattering spectrometer

at 20 °C. A He-Ne laser (10.0 mW at 632.8 nm) was used as a light source. Polymers

were dissolved in 0.1 M NaCl aqueous solution and stirred overnight at 60 °C, then

filtered using a membrane filter with 0.2 μm pores. The angular dependence of the

excess absolute scattering intensity and the difference between the Rayleigh ratio of the

solution and that of the solvent (R_θ) can lead to the weight-average molecular weight

(M_w) and z-average radius of gyration (R_g) estimated from the following relationship:

$KC_p/R_\theta = (1 + R_g^2 q^2/3)/M_w$, where K is the optical constant and q is the magnitude of the

scattering vector. The K value was calculated using $K = 4\pi^2 n^2 (dn/dC_p)^2/N_A \lambda^4$, where n is

the reflective index of the solvent, dn/dC_p is the refractive index increment against C_p,

N_A is Avogadro's number, and λ is wavelength of the light source. The q value was

calculated using $q = (4\pi n/\lambda)\sin(\theta/2)$, where θ is scattering angle. Values of dn/dC_p at

633 nm were determined with an Otsuka Electronics Photal DRM-3000 differential

refractometer at 20 °C. Transmission electron micrograph (TEM) observations were

performed with a JEOL JEM-2100 at an accelerating voltage of 200 kV. Polymers were

dissolved in aqueous solution and stirred overnight at 60 °C. After stirring, the polymer

solutions were maintained at a predetermined temperature for more than one day.

Samples for TEM were prepared by placing one drop of the aqueous solution on a

14

copper grid coated with thin films of Formvar and carbon. Excess water was blotted using filter paper. The samples were stained by sodium phosphotungstate and dried under vacuum for 1 h. The glass transition temperature (T_g) was determined by an SII DSC SSC/5200 differential scanning calorimetry (SDC). The DSC measurements were performed under a continuous flow of dry nitrogen gas. The T_g values were determined in the second heating scan with heating rate of 10 °C/min. Fluorescence emission measurements were performed with a Hitachi F-2500 fluorescence spectrophotometer. C_p was kept constant at 5.0 g/L in a saturated aqueous solution of PNA. The sample solutions were excited at 330 nm, and the excitation and emission slit widths were maintained at 20 and 5.0 nm, respectively. The temperature was decreased from 60 to 10 °C.

3. Results and discussion

After polymerization, percent conversion (x) was monitored using ^{1}H NMR before purification, by comparing integral area ratios between vinyl protons and pendant methylene protons. The M_n(theo) values were calculated using the following equation:

$$M_n(\text{theo}) = \frac{[\text{M}]_0}{[\text{CTA}]_0} \times \frac{x}{100} \times \text{MW}_M + \text{MW}_{CTA} \tag{1}$$

where $[M]_0$ is initial monomer molar concentration, $[CTA]_0$ is initial chain transfer

agent (CTA) molar concentration, MW_M is molecular weight of monomer, and MW_{CTA}

is molecular weight of CTA. The M_n and M_w/M_n values for the polymers used in this

study are summarized in Table 1. The GPC measurements for M_mU_n could not be

performed, because the polymers did not dissolve in the eluents. Therefore, $M_n(GPC)$ of

M_mU_n was calculated using $M_n(GPC)$ of M_mA_n assuming that the pendant amino groups

were completely converted to ureido groups. The M_w/M_n values for M_mA_n are indicated

in Table 1 as are those for M_mU_n. The $M_n(GPC)$ values are only apparent values,

because the standard polymers, poly(sodium styrenesulfonate) and

poly(2-vinylpyridine), were used for the calibrations.

Table 1 Number-average molecular weight (M_n) and molecular weight distribution

(M_w/M_n) of the polymers

| Samples | $M_n(theo)^a$ | $M_n(NMR)^b$ | $M_n(GPC)$ | M_w/M_n |
	$\times 10^{-4}$	$\times 10^{-4}$	$\times 10^{-4}$	(GPC)
PAEM$_{97}$	1.61	-	2.62	1.17
PUEM$_{97}$	1.67	-	2.72^c	1.17^d

16

PMPC$_{20}$	0.618	0.618	0.779	1.13
PMPC$_{95}$	3.22	2.83	1.93	1.15
M$_{20}$U$_{68}$	1.79	1.79	1.11^{c}	1.16^{d}
M$_{20}$U$_{163}$	3.67	3.42	2.94^{c}	1.13^{d}
M$_{95}$U$_{43}$	3.59	3.57	2.40^{c}	1.17^{d}
M$_{95}$U$_{149}$	5.30	5.40	2.99^{c}	1.21^{d}

^{a} Calculated from eqn (1). ^{b} Estimated from ^{1}H NMR. ^{c} Calculated form M_{n}(GPC) of polymers before introduction of ureido groups. ^{d} M_{w}/M_{n} of polymers before introduction of ureido groups.

      The pendant primary amino group in PAEM$_{97}$ was protonated. The ^{1}H NMR signal for PAEM$_{97}$ in D$_{2}$O can be observed at 3.4 ppm attributed to the pendant methylene protons in the vicinity of the protonated amino group (Fig. S3 in the ESI†). The ^{1}H NMR signal for PUEM$_{97}$ in D$_{2}$O can be observed at 3.3 ppm attributed to the pendant methylene protons in the vicinity of the ureido group. It is difficult to confirm introduction of the ureido group to the pendant primary amino group in PAEM$_{97}$ by ^{1}H NMR in D$_{2}$O, because the chemical shifts of the signals in PAEM$_{97}$ and PUEM$_{97}$ were too close. The pendant protonated amino group in PAEM$_{97}$ was converted to the

primary amine under basic conditions. Under basic conditions the pendant methylene protons in the vicinity of the primary amine group in $PAEM_{97}$ can be observed at 2.9 ppm. On the other hand, changes in the chemical shifts for $PUEM_{97}$ cannot be observed by changing the pH. Therefore, ^{1}H NMR spectra for the polymers in 0.1 wt% NaOD containing D_2O were measured to calculate the reaction rate from the pendant amino group to the ureido group. The peak observed at 2.9 ppm in $PAEM_{97}$ under basic conditions completely disappeared after the ureido reaction, i.e., $PUEM_{97}$ was formed. The conversion from the amino group to ureido group was 100% estimated from ^{1}H NMR.
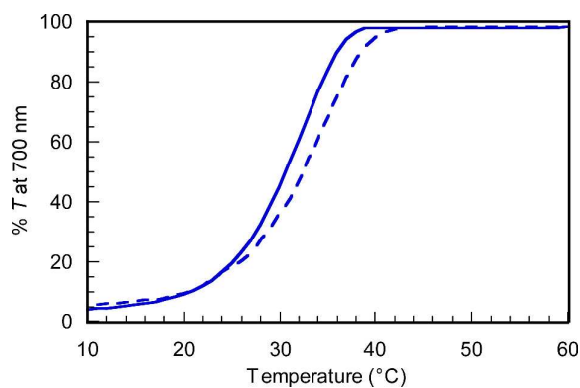
Fig. 2 Percent transmittance (*%T*) at 700 nm for $PUEM_{97}$ in 0.1 M NaCl aqueous solutions as a function of temperature at the polymer concentration (C_p) = 1.0 g/L. Solid (—) and dotted lines (----) indicate cooling and heating processes, respectively.

To determine the UCST of PUEM$_{97}$, changes in percent transmittance (*%T*) were measured as a function of temperature for 0.1 M NaCl aqueous solution in heating and cooling cycles ranging from 10-60 °C (Fig. 2). The *%T* values dropped around a certain temperature in the cooling process. In this study, UCST was defined as an initial point temperature where *%T* begins to drop. The UCST values for the cooling and heating processes were 36 and 40 °C, respectively. A small hysteresis was observed for the cooling and heating processes. The hysteresis of thermo-responsive behavior can often be observed for other UCST-type polymers.[15] We studied molecular weight dependence on thermo-responsive behavior for PUEM$_n$ (Fig. S4 in the ESI†). The UCST value for PUEM$_n$ with low molecular weight was lower than that with high molecular weight.
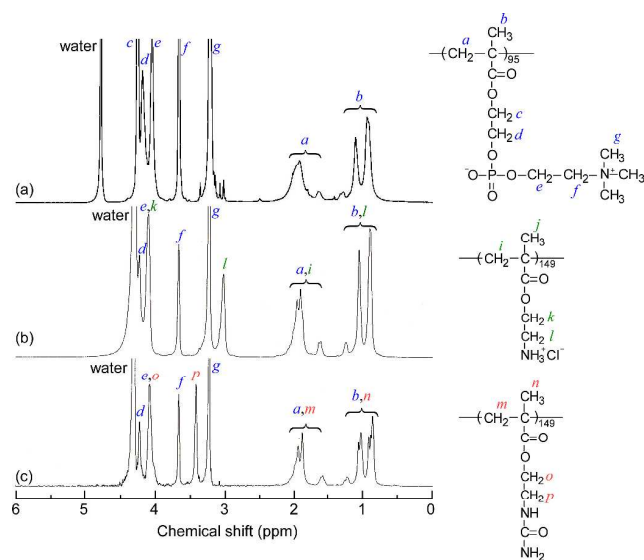
Fig. 3 ^{1}H NMR spectra for (a) PMPC$_{95}$ in D$_2$O at 25 °C, and (b) M$_{95}$A$_{149}$ and (c) M$_{95}$U$_{149}$ in D$_2$O containing 0.1% NaOD at 70 °C.

^{1}H NMR spectra for PMPC$_{95}$ in D$_2$O at 25 °C, and M$_{95}$A$_{149}$ and M$_{95}$U$_{149}$ in D$_2$O containing 0.1% NaOD at 70 °C are shown in Fig. 3. From the ^{1}H NMR spectra for PMPC$_{95}$ in D$_2$O at 25 °C, resonance peaks at 0.8-2.1 ppm are assigned to main chain methyl and methylene protons. The resonance peaks at 3.2 ppm and 3.7-4.5 ppm are attributed to the pendant methyl and methylene protons (Fig. 3a). The ^{1}H NMR spectrum for deprotonated M$_{95}$A$_{149}$ in D$_2$O containing 0.1% NaOD at 70 °C shows signals attributed to the PMPC block and a signal attributed to the pendant methylene protons in the vicinity of a primary amine at 2.9 ppm (Fig. 3b). DP of the PAEM block in M$_{95}$A$_{149}$ was calculated to be 149 from the integral area ratio of the resonance peaks

20

of the pendant methylene protons in PAEM at 2.9 ppm and PMPC at 3.7 ppm. $M_{95}U_{149}$

in D_2O containing 0.1% NaOD at 70 °C shows a resonance peak attributed to the

pendant methylene protons in the vicinity of the primary amine at 3.4 ppm (Fig. 3c).

The conversion from primary amine to ureido groups was estimated as 100%, because

the signal at 2.9 ppm observed in $M_{95}A_{149}$ completely disappeared in $M_{95}U_{149}$.
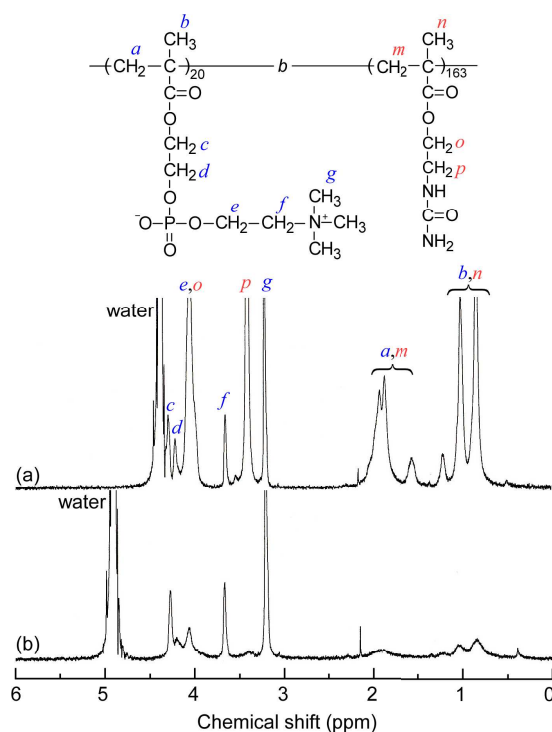
Fig. 4 ^{1}H NMR spectra for $M_{20}U_{163}$ at C_p = 5.0 g/L in D_2O containing 0.1 M NaCl at (a)

60 °C and (b) 10 °C.

To monitor the thermo-responsive association behavior of $M_{20}U_{163}$ in D_2O

containing 0.1 M NaCl, ^{1}H NMR spectra for $M_{20}U_{163}$ at 60 and 10 °C were compared as

shown in Fig. 4. The intensity of the resonance peak due to the pendant methylene

protons in the PUEM block at 3.4 ppm at 10 °C was considerably lower than that at 60

°C. At 60 °C, $M_{20}U_{163}$ can dissolve in D_2O as a unimer state, because 60 °C may be

higher than the UCST for the PUEM block. On the other hand, at 10 °C, $M_{20}U_{163}$

formed micelles composed of a PUEM core and hydrophilic PMPC shell, because the

PUEM block cohered at 10 °C, which may be lower than the UCST. The motion of the

PUEM block was restricted at 10 °C due to the formation of the micelle core. The

intensity of the resonance peaks of PMPC at 3.2 and 3.7 ppm was not affected by

temperature suggesting that the motion of PMPC chains was scarcely influenced by

temperature.
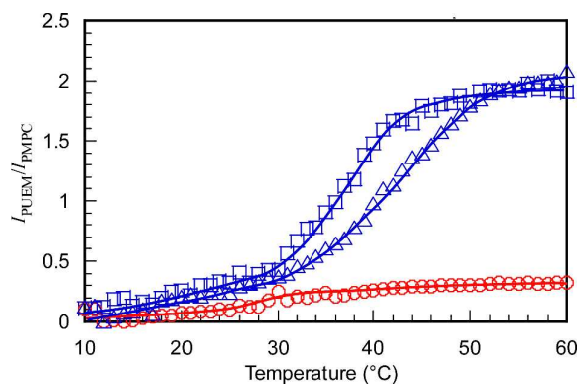
Fig. 5 ^{1}H NMR integrated area intensity ratio (I_{PUEM}/I_{PMPC}) of peaks at 3.4 (I_{PUEM}) and

3.2 ppm (I_{PMPC}) attributed to PUEM and PMPC blocks at C_p = 5.0 g/L as a function of

temperature for $M_{95}U_{149}$ (○) and $M_{20}U_{163}$ (△) in D_2O containing 0.1 M NaCl, and

$M_{20}U_{163}$ (□) in H_2O containing 0.1 M NaCl. The temperature was cooled from 60 to 10

°C.

22

The peak intensity ratios (I_{PUEM}/I_{PMPC}) for pendant methylene protons in the

PUEM block at 3.4 ppm (I_{PUEM}) and pendant methyl protons in the PMPC block at 3.2

ppm (I_{PMPC}) for $M_{95}U_{149}$ and $M_{20}U_{163}$ were plotted against temperature (Fig. 5). When

the temperature decreased from 60 to 10 °C, I_{PUEM}/I_{PMPC} for $M_{95}U_{149}$ gradually

decreased without an inflection point. I_{PUEM}/I_{PMPC} for $M_{20}U_{163}$ in D_2O slightly decreased

above 51 °C, followed by a rapid decrease below 51 °C. In this study, critical

aggregation temperature (T_c) was defined as an initial inflection point temperature

where the intensity ratio started to drop. The motion of the PUEM block in $M_{20}U_{163}$

prevented the formation of a micelle core below 51 °C.

We measured the ^1H NMR spectra for $M_{20}U_{163}$ in H_2O containing 0.1 M NaCl

at 60 and 10 °C (Fig. S5 in the ESI†). I_{PUEM}/I_{PMPC} for $M_{20}U_{163}$ in H_2O containing 0.1 M

NaCl was plotted as a function of temperature (Fig. 5). The temperature was decreased

from 60 to 10 °C. The inflection point, T_c, was observed at 44 °C in H_2O. T_c for $M_{20}U_{163}$

in H_2O estimated from ^1H NMR was 7 °C lower than that in D_2O. It is often observed

that UCST of polymers is higher in D_2O than in H_2O. In particular, UCST is particularly

affected by hydrogen bonding interactions between polymers and aqueous media. An

increase in UCST in D_2O over that in H_2O can be explained by an isotope effect.[34] If an

23

isotope atom is heavier than the original atom, the bonding energy for the isotope atom

is stronger than that for the original atom. UCST in D_2O is higher than that in H_2O,

because the hydrogen bonding interaction of the pendant ureido groups to D_2O

molecules is stronger than that to H_2O.[34]
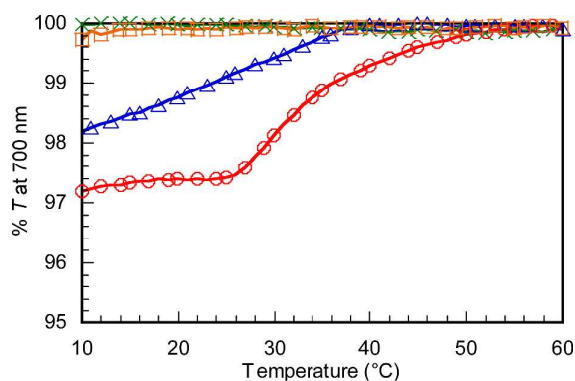
Fig. 6 Percent transmittance (*%T*) at 700 nm for $M_{95}U_{43}$ (□), $M_{95}U_{149}$ (○), $M_{20}U_{68}$ (×),

and $M_{20}U_{163}$ (△) in 0.1 M NaCl aqueous solutions as a function of temperature at C_p =

5.0 g/L. The temperature was decreased from 60 to 10 °C.

The diblock copolymers completely dissolved in 0.1 M NaCl aqueous solutions

at 60 °C. *%T* for the diblock copolymers was plotted as a function of temperature at C_p

= 5.0 g/L (Fig. 6). The temperature was decreased from 60 to 10 °C. The *%T* values for

$M_{95}U_{43}$ and $M_{20}U_{68}$ were practically 100% independent of temperature. These

observations suggest that $M_{95}U_{43}$ and $M_{20}U_{68}$ did not form polymer micelles under these

conditions, because at low temperature, hydrophobicity of the PUEM blocks was not

enough to cause aggregation due to small amounts of the pendant ureido groups in the

block copolymers. $\%T$ for $M_{95}U_{149}$ started to decrease at 49 °C, reaching a

minimum $\%T$ of 9% at 10 °C. $\%T$ for $M_{20}U_{163}$ started to decrease at 41 °C, reaching a

minimum $\%T$ of 98% at 10 °C. The T_c values for $M_{95}U_{149}$ and $M_{20}U_{163}$ were 49 and 41

°C, respectively, estimated from $\%T$. Below T_c, $M_{95}U_{149}$ and $M_{20}U_{163}$ formed polymer

micelles in 0.1 M NaCl aqueous solutions. Cohesive forces of the PUEM blocks in

$M_{95}U_{149}$ and $M_{20}U_{163}$ were enough to form polymer micelles below T_c.
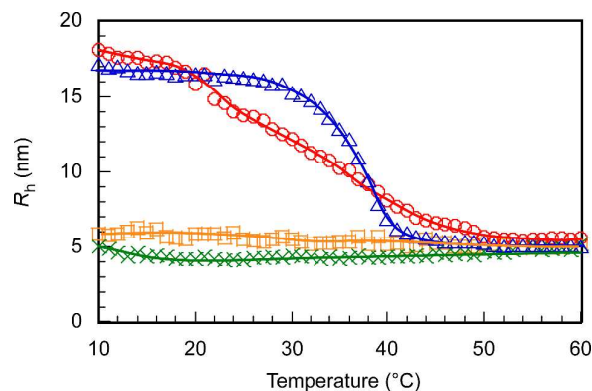
Fig. 7 Hydrodynamic radius (R_h) for $M_{95}U_{43}$ (□), $M_{95}U_{149}$ (○), $M_{20}U_{68}$ (×), and $M_{20}U_{163}$

(△) at C_p = 5.0 g/L in 0.1 M NaCl aqueous solutions as a function of temperature.

R_h values estimated from a cumulant method for 0.1 M NaCl aqueous solutions

of M_mU_n at C_p = 5.0 g/L were plotted as a function of temperature, decreasing from 60

to 10 °C (Fig. 7). The R_h values for $M_{95}U_{43}$ and $M_{20}U_{68}$ were almost constant and

independent of temperature changes. The R_h value for $M_{95}U_{149}$ started to increase below

50 °C, and reached a nearly constant R_h value at 18 nm below 20 °C. T_c (50 °C) for

$M_{95}U_{149}$ estimated from DLS was almost the same as T_c estimated from $\%T$ (Fig. 6). In

the case of $M_{20}U_{163}$, the R_h values started to increase below 42 °C, and the R_h values

were 17 nm below 30 °C, when the temperature decreased from 60 to 10 °C. T_c for

$M_{20}U_{163}$ was 42 °C in 0.1 M NaCl at C_p = 5.0 g/L estimated from the temperature

dependence on R_h, which was almost the same as the value estimated from $\%T$. T_c for

$M_{20}U_{163}$ was 44 °C estimated from ^1H NMR, indicating that the motion of protons in

PUEM started to decrease below 44 °C (Fig. 5). These observations suggested that upon

decreasing the temperature from 60 °C, the PUEM block in $M_{20}U_{163}$ started to form an

intramolecular aggregate within the single polymer chain at 44 °C. Consequently,

intermolecular association of PUEM blocks occurred to form polymer micelles at 42 °C.

R_h distribution data for $M_{95}U_{149}$ and $M_{20}U_{163}$ at 10 and 60 °C estimated from an

NNLS method are shown in Fig. S6 in the ESI†. Unimodal distributions for $M_{95}U_{149}$

and $M_{20}U_{163}$ were observed attributed to unimolecular polymer chains at 60 °C. At 10

°C, bimodal distributions for $M_{95}U_{149}$ were observed attributed to unimers and micelles.

All of the $M_{95}U_{149}$ polymer chains cannot associate at 10 °C, because the PUEM block

was not sufficient to associate and/or the hydrophilicity of the long PMPC block chain

was too strong. On the other hand, at 10 °C, unimodal distribution for $M_{20}U_{163}$ can be

observed attributed to polymer micelles, because $M_{20}U_{163}$ was composed of the

hydrophilic short PMPC block and the long PUEM block, which was a sufficient length

to associate. The R_h distributions for $M_{95}U_{43}$ and $M_{20}U_{68}$ were unimodal independent of

temperature, because these block copolymers did not form micelles (data not shown).

Table 2 Dynamic and static light scattering data for $M_{20}U_{163}$ in 0.1 M NaCl aqueous

solution at 20 °C

	$M_w{}^a \times 10^{-6}$	$R_g{}^a$	$R_h{}^b$	R_g/R_h	$N_{agg}{}^c$	d^d
	(g/mol)	(nm)	(nm)			(g/cm^3)
$M_{20}U_{163}$	3.00	18.2	17.1	1.06	78	0.179

[a] Estimated by SLS in 0.1 M NaCl. [b] Estimated by DLS in 0.1 M NaCl. [c] Aggregation

number of a polymer micelle calculated from M_w of the micelle determined by SLS and

M_w of the corresponding unimers determined by M_n(NMR) and M_w/M_n. [d] Density of

micelles estimated from eqn (2).

SLS measurements were performed at 20 °C (Fig. S7 in the ESI†) to confirm

formation of polymer micelles for $M_{20}U_{163}$. SLS measurements for $M_{95}U_{149}$ micelles

below T_c were not performed because $M_{95}U_{149}$ forms micelles accompanied by

unimolecular polymer chains. The M_w and R_g values for $M_{20}U_{163}$ micelles were

estimated from SLS. It is known that the theoretical value of R_g/R_h for a homogeneous

sphere is 0.778 and it increases substantially for a less dense structure and polydisperse

solution.[35,36] R_g/R_h for $M_{20}U_{163}$ micelles was 1.06, which is close to one, suggesting that

the micelle may be a unimodal spherical shape. Aggregation number (N_{agg}) is defined as

the total number of polymer chains to form one polymer micelle. N_{agg} for $M_{20}U_{163}$

micelle was 78, which was calculated from the apparent M_w value for $M_{20}U_{163}$ micelle

estimated from SLS and M_w for the single polymer chain estimated from M_n(NMR) and

M_w/M_n. The density (d) of micelles can be calculated from the following equation:

$$d = \frac{3M_w}{4\pi N_A R_g^{\ 3}} \qquad (2)$$

The d of $M_{20}U_{163}$ micelle at 20 °C was calculated to be 0.179 g/cm^3. This value is

similar to that for the polyion complex micelles formed from the mixture of

poly(ethylene glycol)-*block*-poly(L-lysine) and poly(ethylene

glycol)-*block*-poly(α,β-asparatic acid).[37] The M_w, R_g, R_h, R_g/R_h, N_{agg}, and d values for

$M_{20}U_{163}$ micelles at 20 °C are summarized in Table 2.
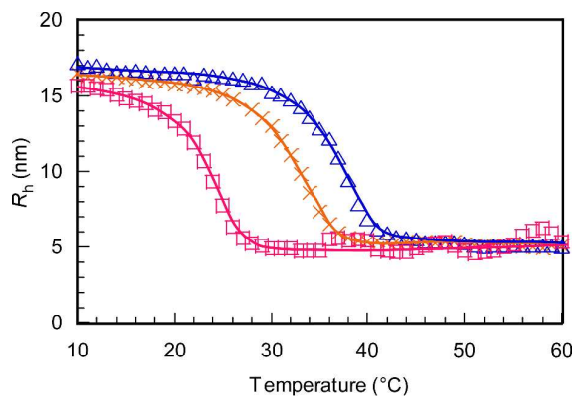
Fig. 8 Hydrodynamic radius (R_h) for $M_{20}U_{163}$ at C_p = 2.5 (□), 4.0 (×), and 5.0 g/L (△) in

0.1 M NaCl aqueous solutions as a function of temperature.

It is reported that the UCST behavior of pendant ureido groups-bearing

poly(allyl amine) depends on C_p.[15] To confirm the effect of C_p for the T_c values of

$M_{20}U_{163}$, the temperature dependence on R_h values was measured at varying C_p (Fig. 8).

When the temperature was decreased from 60 °C, the T_c value, which started to increase

the R_h of $M_{20}U_{163}$ in 0.1 M NaCl, strongly depended on C_P. When the polymer

concentrations were increased to 2.5, 4.0, and 5.0 g/L, the T_c values estimated from

DLS increased to 27, 37, and 42 °C. Below T_c, the R_h values for $M_{20}U_{163}$ were almost

constant at 15-17 nm independent of C_P. The T_c values for $M_{20}U_{163}$ at varying C_P

estimated from DLS were close to the values estimated from the temperature

dependence on %*T* (Fig. S8 in the ESI†).
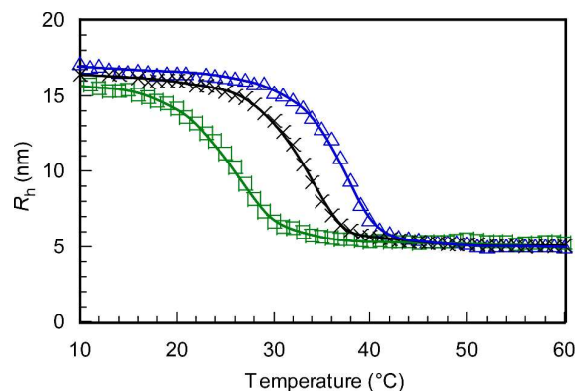
Fig. 9 Hydrodynamic radius (R_h) for $M_{20}U_{163}$ at C_p = 5.0 g/L in aqueous solutions containing 0.1 (△), 0.2 (×), and 0.5 (□) M NaCl as a function of temperature.

To confirm the salt concentration effect for T_c, we measured T_c for aqueous solutions of $M_{20}U_{163}$ at varying NaCl concentrations, when the temperature was decreased from 60 to 10 °C. Temperature dependence on R_h of $M_{20}U_{163}$ at varying NaCl concentrations is shown in Fig. 9. The T_c values decreased with increasing NaCl concentration. The T_c values at the NaCl concentrations of 0.1, 0.2, and 0.5 M were 42, 38, and 31 °C, respectively. The interaction between the pendant ureido groups and water molecules may increase with increasing NaCl concentration presumably due to "salting in" effects. Low molecular weight urea, which has a structure similar to the pendant ureido group, is known to exhibit a strong "salting in" effect.[38] The R_h values at

10 °C were 15-17 nm, almost independent of NaCl concentrations. The T_c values for

$M_{20}U_{163}$ at varying NaCl concentrations estimated from DLS were close to the values

estimated from the temperature dependence on $\%T$ (Fig. S9 in the ESI†).
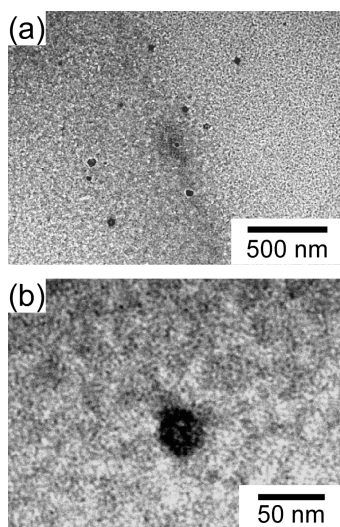
Fig. 10 TEM images of $M_{20}U_{163}$ at different magnifications. The sample for TEM was

prepared at 20 °C.

TEM images for $M_{20}U_{163}$ prepared at 10 °C are shown in Fig. 10. Spherical

shaped objects can be observed. The average radius of the spherical objects was 20.6

nm, which was close to the radii estimated from light scattering measurements. T_g is

important parameter, because T_g is correlative to the polymer micelles dispersed in

water and to the TEM observation. T_g for PMPC homopolymer cannot determined with

DSC according to previous report.[39] DSC measurements for $PUEM_{97}$ and $M_{20}U_{163}$ were

performed to determine the T_g values. The DSC peaks for $PUEM_{97}$ and $M_{20}U_{163}$ were

very weak (Fig. S10 in the ESI†). The T_g for $PUEM_{97}$ and $M_{20}U_{163}$ were similar value,

about 130 °C. This observation indicates that the polymer micelles may be kinetically

frozen, because T_g for the PUEM block was much higher than room temperature.

Therefore, the TEM measurements can be observed for the kinetically frozen micelle

structure.

To confirm that the core of the polymer micelles formed below their T_c can

incorporate hydrophobic small guest molecules, we performed fluorescence studies

using PNA as a fluorescence probe. It is known that the fluorescence intensity of PNA

increases and the maximum fluorescence wavelength (λ_{max}) shifts to shorter wavelength

when PNA molecules are in a hydrophobic microenvironment.[40] The fluorescence

intensity and λ_{max} of PNA in 0.1 M NaCl aqueous solutions at 10 and 60 °C did not

change in the absence of the polymers. In the presence of 5.0 g/L of polymers, the

fluorescence intensity increased and λ_{max} shifted to shorter wavelength at 60 °C

compared to those at 10 °C (Fig. S11 in the ESI†). These observations suggest that PNA

molecules were incorporated in the PUEM core of the micelles at 10 °C.
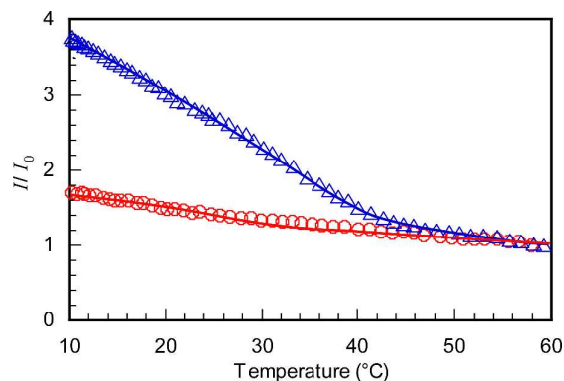
Fig. 11 Normalized fluorescence intensity ratio (I/I_0) of PNA in the presence of 5.0 g/L

of $M_{95}U_{149}$ ($\circ$) and $M_{20}U_{163}$ ($\triangle$) in 0.1 M NaCl aqueous solutions as a function of

temperature. I is the intensity in the presence of the polymer at the temperature, and I_0 is

the intensity in the absence of the polymer at room temperature.

It was difficult to determine the exact λ_{max} under these experimental conditions,

because the fluorescence spectra of PNA were broad. Therefore, we monitored only the

fluorescence intensity of PNA. The fluorescence intensity ratios (I/I_0) were plotted as a

function of temperature in the presence of the polymers (Fig. 11). I is the intensity at the

temperature, and I_0 is the intensity in the absence of the polymer at room temperature.

As the temperature decreased from 60 °C, I/I_0 for $M_{20}U_{163}$ began to increase at 43 °C,

which is similar to the value of T_c estimated by DLS measurements. Below the T_c, the

PNA molecules were incorporated into the PUEM core of the $M_{20}U_{163}$ micelles. The I/I_0

values in the case of $M_{95}U_{149}$ and $M_{20}U_{163}$ at 10 °C were 1.7 and 3.8 times larger than

33

those at 60 °C. The PMPC block in $M_{95}U_{149}$ is longer than that in $M_{20}U_{163}$. The PUEM

block in $M_{95}U_{149}$ is shorter than that in $M_{20}U_{163}$. Therefore, the core of the polymer

micelle formed from $M_{20}U_{163}$ below T_c should be more hydrophobic than that formed

from $M_{95}U_{149}$. At 10 °C, $M_{95}U_{149}$ formed polymer micelles accompanied by

unimolecular chains, because a bimodal R_h distribution was observed (Fig. S6 in the

ESI†). The associative nature of the PUEM block in $M_{95}U_{149}$ below T_c was weak due to

low dehydration of the pendant ureido groups. I/I_0 for $M_{95}U_{149}$ at 10 °C was only 1.7

times larger than that at 60 °C, presumably because the core of $M_{95}U_{149}$ micelles was

not hydrophobic enough to incorporate hydrophobic PNA molecules. On the other hand,

almost all $M_{20}U_{163}$ chains formed polymer micelles at 10 °C, because a unimodal R_h

distribution attributed to the polymer micelle can be observed. I/I_0 for $M_{20}U_{163}$ at 10 °C

was 3.8 times larger than that at 60 °C, because hydrophobic PNA molecules can be

incorporated into the sufficiently hydrophobic core of $M_{20}U_{163}$ micelles. The I/I_0 value

of PNA incorporated into amphiphilic polymer aggregates formed from

cholesterol-modified pullulan derivative (CHP) are reported to be about 100 in water.[41]

The I/I_0 value of PNA in $M_{20}U_{163}$ polymer micelles was considerably smaller than that

in the conventional micelles, suggesting that the cores of $M_{20}U_{163}$ polymer micelles are

more hydrophilic than the cores in conventional polymer micelles. Polymer micelle

formation at $< T_c$ may be driven by hydrogen bonding interactions between the pendant

ureido groups in PUEM blocks.

Table 3 Critical aggregation temperature (T_c) for $M_{20}U_{163}$ and $M_{95}U_{149}$ at $C_p = 5.0$ g/L in

0.1 M NaCl aqueous solutions

Samples	T_c (°C)			
	NMR[a]	% T	R_h	fluorescence
$M_{20}U_{163}$	44	41	42	43
$M_{95}U_{149}$	-	49	50	-

[a] Estimated from ^{1}H NMR measured in H_2O containing 0.1 M NaCl.

The T_c values for $M_{20}U_{163}$ and $M_{95}U_{149}$ estimated from NMR, %T, light

scattering, and fluorescence probe techniques are summarized in Table 3 in 0.1 M NaCl

at $C_p = 5.0$ g/L. The T_c values for $M_{20}U_{163}$ and $M_{95}U_{149}$ were 41-44 °C and 49-50 °C,

respectively.
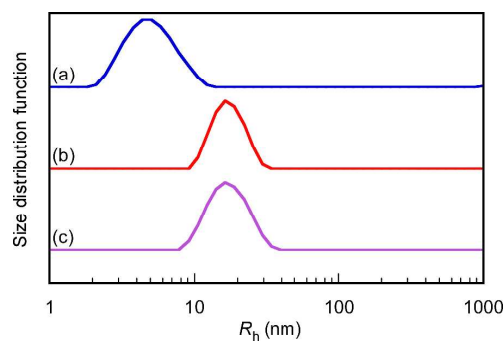
Fig. 12. Hydrodynamic radius (R_h) distributions for (a) BSA (1 g/L), (b) $M_{20}U_{163}$ (5 g/L), and (c) $M_{20}U_{163}$ (5 g/L) in the presence of BSA (1 g/L) in PBS at 20 °C.

Interaction between $M_{20}U_{163}$ micelle and BSA was studied using a DLS technique. It is expected that protein such as BSA cannot interact with $M_{20}U_{163}$ micelle because the micelle was covered with biocompatible PMPC chains. Typical R_h distributions for BSA, $M_{20}U_{163}$ micelle, and $M_{20}U_{163}$ micelle in the presence of BSA in PBS buffer at 20 °C are shown in Fig. 12. Each R_h distribution indicates unimodal. The R_h values for BSA and $M_{20}U_{163}$ micelle were 5.3 and 17.4 nm, respectively. The R_h value for $M_{20}U_{163}$ micelle in PBS was similar to that (R_h = 17.1 nm) in 0.1 M NaCl. The R_h distribution for $M_{20}U_{163}$ micelle in the presence of BSA was unimodal with R_h = 17.5 nm. The size and distribution of $M_{20}U_{163}$ micelle (5 g/L) was scarcely affected by BSA (1 g/L). This observation suggests that there is no interaction between $M_{20}U_{163}$ micelles and BSA. The scattering intensities for BSA and $M_{20}U_{163}$ micelles were 402 Kcps and 29.4 Mcps, respectively. The R_h distribution for BSA was disappeared in the presence of $M_{20}U_{163}$ micelles, because the scattering intensity of the micelles was about 73 times higher than that of BSA.

36

4. Conclusions

Pendant ureido groups-bearing homopolymer, PUEM, was prepared via RAFT radical polymerization and post-modification reaction. PUEM exhibited UCST type phase transition below 36 °C in 0.1 M NaCl aqueous solutions. The diblock copolymers, M_mU_n, were also prepared via RAFT radical polymerization and post-modification reaction. $M_{95}U_{149}$ and $M_{20}U_{163}$ were dissolved in 0.1 M NaCl as a unimer state at $> T_c$. The T_c values for $M_{95}U_{149}$ and $M_{20}U_{163}$ were 41-44 °C and 49-50 °C, respectively. Below the T_c, these diblock copolymers formed polymer micelles comprising a PUEM core and hydrophilic PMPC shell. The T_c values can be controlled by the polymer concentrations and the concentration of added salt. It is expected that the UCST-type thermo-responsive polymer micelles can be applied as a carrier for DDS, because the polymer micelles can incorporate hydrophobic guest molecules with controlled-release, and their surface is covered with biocompatible PMPC shells.

Devices (No. 2013B25).

References

1   W. Sun, S. Zhou, B. You and L. Wu, *Macromolecules*, 2013, **46**, 7018–7026.

2   Y. Zhao, *Macromolecules*, 2012, **45**, 3647–3657.

3   Y. Osada, and J.-P. Gong, *Adv. Mater.*, 1998, **10**, 827–837.

4   H. Mori, A. H. E. Müller and J. E. Klee, *J. Am. Chem. Soc.*, 2003, **125**, 3712–3713.

5   N. Nath and A. Chilkoti, *Adv. Mater.*, 2002, **14**, 1243–1247.

6   A. S. Hoffman, P. S. Stayton, V. Bulmus, G. Chen, J. Chen, C. Cheung, A. Chilkoti,

    Z. Ding, L. Dong, R. Fong, C. A. Lackey, C. J. Long, M. Miura, J. E. Morris, N.

    Murthy, Y. Nabeshima, T. G. Park, O. W. Press, T. Shimoboji, S. Shoemaker, H. J.

    Yang, N. Monji, R. C. Nowinski, C. A. Cole, J. H. Priest, H. J. Milton, K. Nakamae,

    T. Nishino and T. Miyata, *J. Biomed. Mater. Res.*, 2000, **52**, 577–586.

7   D. Schmaljohann, *Adv. Drug Delivery Rev.*, 2006, **58**, 1655–1670.

8   N. Matsuzaka, M. Nakayama, H. Takahashi, M. Yamato, A. Kikuchi and T. Okano,

    Biomacromolecules, 2013, **14**, 3164–3171.

9   S. Wiktorowicz, H. Tenhu and V. Aseyev, *Macromolecules*, 2013, **46**, 6209–6216.

10 S. Ansgar, K. Oliver and A. R. M. Michael *Macromolecules*, 2013, **46**, 6031–6037.

11 G. B.H. Chua, P. J. Roth, H. T. T. Duong, T. P. Davis and A. B. Lowe, *Macromolecules*, 2012, **45**, 1362–1374.

12 M. Dan, Y. Su, X. Xiao, L. Li and W. Zhang, *Macromolecules*, 2013, **46**, 3137–3146.

13 P. A. Woodfield, Y. Zhu, Y. Pei and P. J. Roth, *Macromolecules*, 2014, **47**, 750–762.

14 J. Seuring and S. Agarwal, *Macromolecules*, 2012, **45**, 3910–3918.

15 N. Shimada, H. Ino, K. Maie, M. Nakayama, A. Kano and A. Maruyama, *Biomacromolecules*, 2011, **12**, 3418–3422.

16 N. Shimada, M. Nakayama, A. Kano and A. Maruyama, *Biomacromolecules*, 2013, **14**, 1452–1457.

17 P. C. Weber, J. J. Wendoloski, M. W. Pantoliano and F. R. Salemme, *J. Am. Chem. Soc.*, 1992, **114**, 3197–3200.

18 H. B. Robert *J. Am. Chem. Soc.*, 1983, **105**, 2776–2783.

19 G. Jakli and W. A. Van Hook, *J. Phys. Chem.*, 1981, **85**, 3480–3493.

20 G. C. Kresheck and H. A. Scheraga, *J. Phys. Chem. B*, 1965, **69**, 1704–1706.

21 J. Grdadolnik and Y. Marehal, Y. *J. Mol. Struct.*, 2002, **615**, 177–189.

22 D. Wang, J. Yin, Z. Zhu, Z. Ge, H. Liu, S. P. Armes and S. Liu, *Macromolecules*,

2006, **39**, 7378−7385.

23   J. Xuan, O. Boissiere, Y. Zhao, B. Yan, L. Tremblay, S. Lacelle, H. Xia and Y.

Zhao, *Langmuir*, 2012, **28**, 16463−16468.

24   S. Yusa, S. Yamago, M. Sugahara, S. Morikawa, T. Yamamoto and Y. Morishima,

Macromolecules, 2007, **40**, 5907−5915.

25   S. Dai, P. Ravi, K. C. Tam, B. W. Mao and L. H. Gan, *Langmuir*, 2003, **19**,

5175−5177.

26   H. Zhang, X. Tong and Y. Zhao, *Langmuir*, 2014, **30**, 11433–11441.

27   T. Ueda, H. Oshida, K. Kurita, K. Ishihara and N. Nakabayashi, *Polym. J.*, 1992,

24, 1259−1269.

28   Y. Iwasaki and K. Ishihara, *Sci. Technol. Adv. Mater.*, 2012, **13**, 064101.

29   Y. Iwasaki and K. Ishihara, *Anal. Bioanal. Chem.*, 2005, **381**, 534−546.

30   K. Ishihara, T. Ueda and N. Nakabayashi, *Polym. J*, 1990, **22**, 355−360.

31   Y. Mitsukami, M. S. Donovan A. B. Lowe and C. L. McCormick, *Macromolecules*,

2001, **34**, 2248−2256.

32   D. E. Koppei, *J. Chem. Phys.*, 1972, **57**, 4814−4820.

33   K. Huber, S. Bantle, P. Lutz and W. Buchard, *Macromolecules*, 1985, **18**,

1461−1467.

34   N. Endo, H. Shirota and K. Horie, *Macromol. Rapid Commun.*, 2001, **22**, 593−597.

35   T. Konishi, T. Yoshizaki and H. Yamakawa, *Macromolecules*, 1991, **24**, 5614−5622.

36   E. Nordmeier and M. D. Lecher, *polym. J.*, 1989, **21**, 623−632.

37   A. Harada and K. Kataoka, *Macromolecules*, 1995, **28**, 5294–5299.

38   R. Zangi, R. Zhou and B. J. Berne, *J. Am. Chem. Soc.*, 2009, **131**, 1535–1541.

39   Y. Inoue, J. Watanabe, M. Takai, S. Yusa and K. Ishihara, *J. Polym. Sci., Part A: Polym. Chem.*, 2005, **43**, 6073−6083.

40   M. Ikemi, N. Odagiri, S. Tanaka, I. Shinohara and A. Chiba, *Macromolecules*, 1982, **15**, 281−286.

41   K. Akiyoshi, S. Deguchi, N. Moriguchi, S. Yamaguchi and J. Sunamoto, *Macromolecules*, 1993, **26**, 3062−3068.

Graphical Abstract

Ureido groups-bearing methacrylate-type polymer shows an upper critical solution temperature in water. We prepared a thermo-responsive diblock copolymer composed of a ureido groups-bearing block and a biocompatible hydrophilic phosphorylcholine groups-bearing block.

1